



## Research article

## Optimization of the photocatalytic degradation process of aromatic organic compounds applied to mangrove sediment



Marcio J. Silva<sup>a,\*</sup>, Sarah A.R. Soares<sup>b</sup>, Ingrid D.F. Santos<sup>b</sup>, Iuri M. Pepe<sup>c</sup>, Leandro R. Teixeira<sup>c</sup>, Lucas G. Pereira<sup>c</sup>, Lucas B.A. Silva<sup>c</sup>, Joil J. Celino<sup>a</sup>

<sup>a</sup> Postgraduate Program in Geochemistry: Petroleum and Environment, Geoscience Institute, Federal University of Bahia, Rua Barão de Jeremoabo, s/n, 40170-020 Salvador, BA, Brazil

<sup>b</sup> LEPETRO, Excellence in Geochemistry: Petroleum, Energy and Environment, Geoscience Institute, Federal University of Bahia, Rua Barão de Jeremoabo, s/n, 40170-020 Salvador, BA, Brazil

<sup>c</sup> Laboratory of Optical Properties, Institute of Physics, Federal University of Bahia, Rua Barão de Jeremoabo, s/n, 40170-020 Salvador, BA, Brazil

## ARTICLE INFO

## Keywords:

Chromatography  
Chemometrics  
Physical chemistry  
Environmental analysis  
Environmental geochemistry  
Environmental pollution  
Photodegradation  
Advanced oxidative processes  
Heterogeneous photo catalysis  
Experimental design  
Multiple response

## ABSTRACT

Polycyclic aromatic hydrocarbons (PAHs) are part of a class of organic compounds resistant to natural degradation. In this way, heterogeneous photocatalysis becomes useful to degrade persistent organic pollutants, however it can be influenced by environmental variables (i.e.: organic matter) and experimental factors such as: mass of the photocatalyst and irradiation time. The objective of this research was to use a factorial design  $2^k$  as a function of the multiple response (MR) to evaluate simultaneously experimental conditions for the photo-degradation of polycyclic aromatic hydrocarbons in contaminated mangrove sediment and its application in oil from Potiguar Basin in Brazil. The sediment samples collected in Belmonte city (Southern Bahia state) were contaminated with 0.25 mg kg<sup>-1</sup> of Acenaphthene, Anthracene, Benzo[a]Anthracene, Indene[1,2,3cd]pyrene, Dibenzo[ah]anthracene, Benzo[ghi]pyrene. Factors such as mass of the photocatalyst and irradiation time were evaluated in factorial design  $2^2$ , with triplicate from the central point, to 1g of the PAH contaminated sediment. After performing the experiments, it was found that the best experimental condition for the degradation of all PAHs indicated by MR was the central point (0.5 g of photocatalyst and 12h of irradiation). For such conditions, the half-life of PAHs varied from 3.51 to 9.37 h and the degradation speed constant between 0.0740 to 0.1973 h<sup>-1</sup>. The comparison of the optimized methodology between photolysis tests and heterogeneous photocatalysis was performed using the Kruskal-Wallis test, which indicated a difference for the reference solution, where heterogeneous photocatalysis was more efficient in the degradation of PAHs. The optimized methodology was apply in samples contaminated with crude oil from Potiguar Basin, no significant difference was observed in the aromatic fraction, using for the Kruskal-Wallis test. Heterogeneous photocatalysis has shown to be a promising remediation technique to remedy aromatic organic compounds in mangrove sediments.

## 1. Introduction

Polycyclic aromatic hydrocarbons (PAHs) belong to a class of organic compounds persistent or recalcitrant to natural degradation. These compounds pose risks to human health and natural ecosystems, due to their carcinogenic, mutagenic and genotoxic properties. The high hydrophobicity of PAHs promotes a strong association with organic matter contained in mangrove sediments (Bolden et al., 2017; Singh et al., 2016; Kuppasamy et al., 2017; Abdel-Shafy and Mansour, 2016; Jia et al., 2012). Therefore, remediation techniques must be applied to remove

PAHs in the mangrove ecosystem. In this context, advanced oxidative processes (OAPs) can be used to remove organic pollutants.

OAPs cause structural changes in the pollutant by modifying its reactivity, distribution and residence time in the environment due to a series of chemical reactions triggered by the formation of hydroxyl radicals ( $\bullet$ OH). The high reactivity of  $\bullet$ OH (oxidizing agent,  $E^\circ = 2.8$  V) gives the condition to attack a variety of organic compounds. Among the POAs, heterogeneous photocatalysis uses a semiconductor acting as a catalyst to generate hydroxyl radicals (Ahmed et al., 2011). Semiconductors form permitted bands of energies called the valence band

\* Corresponding author.

E-mail address: [msilva.quimica@gmail.com](mailto:msilva.quimica@gmail.com) (M.J. Silva).

<https://doi.org/10.1016/j.heliyon.2020.e05163>

Received 19 May 2020; Received in revised form 6 August 2020; Accepted 1 October 2020

2405-8440/© 2020 The Authors. Published by Elsevier Ltd. This is an open access article under the CC BY-NC-ND license (<http://creativecommons.org/licenses/by-nc-nd/4.0/>).

(VB) and conduction band (CB). As well, a prohibited band of energy with no electrons called a “band-gap”, (Eg) (Marquès et al., 2016).

In the process of pollutant degradation by heterogeneous photo catalysis, some semiconductors have been used. However, titanium dioxide (TiO<sub>2</sub>) is the most used, due to its photo stability, low cost, low toxicity and among other advantages (Gaya and Abdullah, 2008; Ahmed et al., 2011). Heterogeneous photocatalysis is widely used in aqueous systems and there are few studies regarding the photocatalytic degradation of organic pollutants, such as PAHs, on the surface of soils and sediments (Marquès et al., 2016).

The photodegradation of organic pollutants in soils is affected by several factors such as: composition and size of the constituent particles of the soil, thickness of the layer that will be irradiated, intensity of light, quantity of humic substances and moisture content (Balmer et al., 2000; Jia et al., 2012; Gupta and Gupta, 2015; Marquès et al., 2016). According to Dong et al. (2010) photocatalytic degradation is an effective process to eliminate PAHs in a solid phase. However, the dosage of the photocatalyst in the contaminated soil sample affects the rate of degradation of the organic pollutant, as well as the amount of hydrogen peroxide (H<sub>2</sub>O<sub>2</sub>).

In order to evaluate the effects of factors on the degradation process of organic pollutants, techniques of experimental design can be employed. The use of experimental design can assist in the selection of factors that directly influence the photodegradation of organic pollutants, as well as optimize methodologies for the photocatalytic degradation process (Ambrosio et al., 2017; Andrade Neto et al., 2017; Barka et al., 2014; Guz et al., 2017). The basic principle of experimental design is related to experiments associated with a composite matrix with different combinations of the levels (lower and upper) of the factors studied (Novaes et al., 2017). With the variation of the factors levels is possible to calculate the main effects and their interactions, to select significant factors in the process and to indicate the conditions to obtain the best answer (Cox and Reid, 2000; Calado and Montgomery, 2003). In processes that have more than one analytical signal (variable of interest) it is essential to apply the function desirability or multiple response, as it will indicate the best experimental conditions to obtain the maximization or minimization of more than one response simultaneously (Ferreira, 2015).

The objective of this work was to use an experiment technique associated with the multiple response (MR) to evaluate simultaneous experimental conditions for some PAHs photodegradation and its application in mangrove sediment samples contaminated by crude oil from basin Potiguar, Brazil.

## 2. Materials and methods

### 2.1. Reagents, solutions and samples

The particle size analysis was performed in a laser diffraction particle analyzer (Cilas, model 1064, Orléans, France). The organic matter content in sediment was oxidize with hydrogen peroxide 30%, H<sub>2</sub>O<sub>2</sub> (P.A., Merck, Darmstadt, Germany) in a digesting block (MA 4025, Marconi, São Paulo, Brazil). Then sodium hexametaphosphate solution, (NaPO<sub>3</sub>)<sub>6</sub>, 0.1 mol L<sup>-1</sup> (P.A., Neon, São Paulo, Brazil) was added to avoid flocculation (EMBRAPA, 2017). GRADISTAT software version 5.0<sup>®</sup>, developed by Simon Blott (London University), was used for data processing.

Total organic carbon (TOC) was determined using the methodology of the Brazilian Agricultural Research Corporation (EMBRAPA, 2017). About 1 g of sediment was decarbonized with hydrochloric acid solution (HCl, Merck, Darmstadt, Germany) 1 mol L<sup>-1</sup> to remove inorganic carbon and washed in distilled water at 80 °C until the total removal of the chloride ions. The silver nitrate solution 1% (m v<sup>-1</sup>), AgNO<sub>3</sub> P.A. (Fmaia, Belo Horizonte, Brazil) was used to verify that the chloride ion was eliminated from the sample, if this ionic species remained, the washing with distilled water is repeated. Then, the sample were analyze in the elementary analyzer (628CN, LECO, Rio de Janeiro, Brazil).

Approximately 50 g of sediment and 150 mL of dichloromethane (Merck, Darmstadt, Germany) were used for four hours in a soxhlet system to extract the soluble organic fraction. Then, this treated sediment was stored in a glass container and used during the experiments. Another part of this sediment was fortified with 25 mL of a standard solution containing the PAHs (Acenaphthylene (AcNf), Acenaphthene (AcN), Anthracene (AN), Benzo[a]Anthracene (BaA), Indene[1,2,3 cd]Pyrene (IP), Dibenzo[ah]Anthracene (DahA), Benzo[ghi]Pyrene (BghiP)) 500 µg L<sup>-1</sup> in methanol, with the final concentration of PAHs in the sediment 0.25 mg kg<sup>-1</sup>.

The proposed methodology was apply in mangrove sediment samples contaminated with crude oil from basin Potiguar, provided by the company PETROBRAS S.A. Approximately 26 mg of the oil was weighed in a petri dish. Then, was added 2 mL of dichloromethane (Merck, Darmstadt, Germany) and 1 g of the sediment was mixed in the solution until the solvent evaporate. This contamination procedure was performed for the photo-oxidation experiments in the presence or absence of the photocatalyst.

### 2.2. Photocatalyst

The titanium dioxide (TiO<sub>2</sub>) photocatalyst was provided by Evonik company, commercially available as Degussa P-25, consisting of 80% of the anatase phase and 20% of the rutile phase, with 50 m<sup>2</sup> g<sup>-1</sup> surface area. This photocatalyst was used without any type of treatment or structural alteration.

### 2.3. Reactor system

The PAHs photodegradation experiments were carried out in a photochemical reactor system built at the Laboratory of Optical Properties (LaPO), located at Physics Institute - Federal University of Bahia (link: <http://www.fis.ufba.br/laboratorio-de-propriedades-oticas-lapo>). The reactor consists in a ultraviolet radiation source, composed of 13 LEDs emitting light at 365 nm. This light source was placed inside a wooden box 80 x 53 cm with the internal walls covered with a black film. The equipment also has a current source ranging 0–60 mA and a multimeter to measure the current generated. The wavelength emitted by the LEDs has the energy necessary for the activation of the photocatalyst. Figure 1 represents the reactor system used in PAHs photodegradation experiments.

### 2.4. Multivariate optimization

Table 1 shows the factors and the levels (low, high and central point) with real and coded values. The experiments were carried out in 60 ×

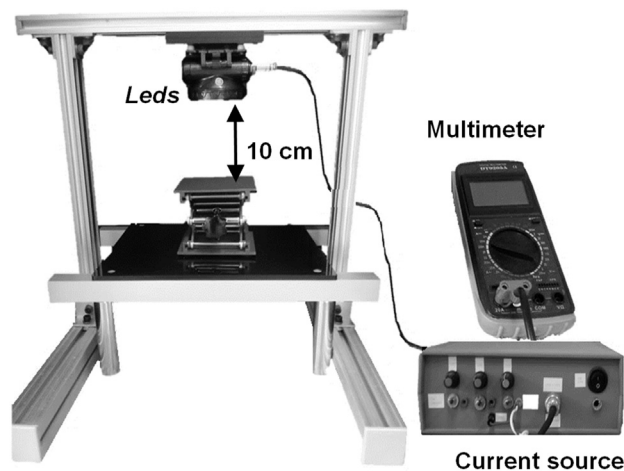


Figure 1. Schematic representation of the photochemical reactor used in the PAHs photo degradation process.

**Table 1.** Factors and levels used for factorial design  $2^2$  in the study of PAH photo degradation in mangrove sediment. The values -1, 0 and +1 represent the coded levels.

Factors	-1	0	+1
Mass of photo catalyst (g)	0.2	0.5	0.8
Irradiation time (hours)	10	12	14

15mm glass petri dishes. 1g of wet mangrove sediment with 2mL of deionized water from the Milli-Q<sup>®</sup> system (Millipore Corporation), forming a thin thickness.

The proposed planning matrix was built using free software R, version 3.6.0 (R Development Core Team, 2019) with the Rstudio interface in version 1.1.463 (RStudio Team, 2015) using the quality Tools package (Roth, 2016). The interpretation of the results and the construction of the Pareto graphic were performed with the same package. The planning scripts are arranged in the supplementary material.

### 2.5. PAH extraction

After photodegradation, the samples were dried in the freeze dryer (LI08, Liotop, São Carlos, Brazil). Then, 1g sample was transferred to Teflon tubes, add 25 mL of the n-hexane/acetone PA 1:1 ( $v v^{-1}$ ) (Merck, Darmstadt, Germany) extraction solution and a magnetic bar. The PAHs extraction carried out by EPA 3546 (US EPA, 2007a) in a closed microwave oven (Multiware PRO, Anton PAAR, Graz, Austria) at 110 °C for 25 min. After cooling, the extract was dried on a rotary evaporator (R-201/215, BÜCHI, Flawil, Switzerland) to 1 mL and transferred to a 1.8 mL vial. The extracts were analyzed by gas chromatography mass spectrometer (GC-MS).

### 2.6. PAH quantification

The quantification of PAHs was performed by EPA 8270-D (US EPA, 2007b) using a gas chromatography mass spectrometer (GC-MS 7890B, with automatic sampler 7693 and mass detector 5977A, Agilent Technologies, Santa Clara, California, United States). The equipment operated in selected ion monitoring mode (SIM), using a fused silica capillary column DB-5 MS (60 m × 250  $\mu$ m × 0.25  $\mu$ m). The analysis conditions were: oven temperature 50 °C, heating from 60 to 310 °C with 2 °C/min heating ramp, remaining for 10 min; injector temperature at 300 °C and detector temperature at 330 °C; helium carrier gas at 30 mL  $min^{-1}$ , constant flow; 1 $\mu$ L injection volume.

The PAH photodegradation percentage was obtained applying Eq. (1).

$$\% = \left( \frac{C_0 - C_f}{C_0} \right) \times 100 \quad (1)$$

where,  $C_0$  is individual PAH concentration in non-irradiated sediment sample,  $C_f$  is the concentration of the same PAH in sample after photodegradation.

### 2.7. Kinetic study of PAH photodegradation

The methodology proposed by Mishra et al. (2017) and Nugraha and Fatimah (2013), with modifications, was applied. In a petri dish, 10 g of mangrove sediment fortified with standard PAHs solution, 0.5 g of the photocatalyst and 7 mL of deionized water were added. The samples were photodegraded 0, 4, 8, 12, 24 and 30 h and 1 g of sample was taken and prepared and analyzed according to the protocol described in item (2.6).

Eqs. (2) and (3) were used to determine the half-life of PAHs in the heterogeneous photocatalysis process.

$$\frac{\ln C_0}{C_i} = k.t \quad (2)$$

$$t_{1/2} = \frac{\ln 2}{k} = \frac{0,6931}{k} \quad (3)$$

where,  $C_0$  is individual PAH concentration in the sediment sample,  $C_i$  is concentration from the same PAH after photodegradation,  $t$  is the exposure time (in hours),  $t_{1/2}$  is the half-life of the individual PAH,  $k$  is the reaction constant of the pseudo first order ( $h^{-1}$ ).

### 2.8. Photolysis experiments in petroleum and in the reference solution

The photolysis experiments with sediment contaminated with oil or with the reference solution with PAHs were carried out in glass petri dishes. 1 g of sediment was used, moistened with 2 mL of deionized water, forming a very thin thickness of the mixture and irradiated for 12 h. The results of these experiments were compared with the results of heterogeneous photocatalysis to evaluate the efficiency of the photocatalyst  $TiO_2$ .

### 2.9. Petroleum fractionation by liquid chromatography

The fractionation of petroleum samples after degradation was performed by open column liquid chromatography (30 × 2 cm) filled with 4 g of silica gel (60 mesh size, Merck, Darmstadt, Germany) in n-hexane (Merck, Darmstadt, Germany) and about 26 mg of sample.

The n-alkane fraction was eluted using 30 mL of n-hexane. The aromatic fraction was eluted using 40 mL of n-hexane/dichloromethane 4:1 ( $v v^{-1}$ ) mixture (Merck, Darmstadt, Germany). The fraction containing nitrogen, sulfur and oxygen compounds (NSO) was eluted with 40 mL of dichloromethane/methanol 4:1 ( $v v^{-1}$ ) mixture (Merck, Darmstadt, Germany). The fractions were reduced in a rotary evaporator until 250  $\mu$ L (R-201/215, BÜCHI, Flawil, Switzerland) and transferred to a 1.8 mL vial. Only the aromatic fraction was analyzed.

### 2.10. Statistical analysis

Statistical analyzes were performed using free software R, version 3.6.0 (R Development Core Team, 2019) with the Rstudio interface in version 1.1.463 (RStudio Team, 2015). With the results of the photocatalytic degradation of the aromatic organic compounds, the Shapiro-Wilk test with the base function of the Rstudio *shapiro.test()* was applied to verify that the results follow a normal distribution. However, the results do not follow a normal distribution, requiring use non-parametric tests.

For comparison between the process of photocatalytic degradation and photolysis, the Kruskal Wallis test was applied with the base function of Rstudio *kruskal.test()*, a non-parametric test, analogous to ANOVA, to compare two or more independent samples. The null hypothesis,  $H_0$ , predicts that the samples come from the same population with the same distribution format (Virgillito, 2006). The Nemenyi multiple comparison test (analogous to the Tukey test) which consists of a comparison analysis in pairs with the aim of verifying whether the factors differ from each other. This test was applied using the *posthoc.kruskal.nemenyi.test()* function using the PMCMR package (Pohlert, 2014). The scripts of these analyzes are arranged in the complementary material.

#### 2.10.1. Generalized linear model

The relationship between the random variable of interest and the set of explanatory or exploratory variables was determined using the generalized linear model (GLM). This type of regression was used because the assumption of normality of the variables was not met for the results of the photocatalytic degradation of aromatic organic compounds. Modeling a response variable according to a set of independent variables

means obtaining the contribution of each independent variable over the response variable.

GLM was proposed by [Nelder and Wedderburn \(1972\)](#). This model assumes that the variable of interest has a distribution belonging to the exponential family. Because of this, there is greater flexibility between the mean of the variable of interest and the linear predictor  $\eta$ . The GLM is an extension of the linear regression models, as they have a linear structure and consists of three components ([Eguchi, 2017](#); [Cordeiro and Andrade, 2009](#) [Gracindo et al., 2011](#)):

- random component represented by a set of independent values  $Y_1, Y_2, \dots, Y_n$  with distribution belonging to the exponential family;
- systematic component enters the model as the linear sum of the effects of the explanatory variables that is given by;

$$\eta_i = \sum_{r=1}^p x_{ir} \beta_j = x_i^T \beta \text{ ou } \eta = X\beta$$

where  $X = (x_1, \dots, x_n)^T$  the model matrix,  $\beta = (\beta_1, \dots, \beta_p)^T$  the parameter vector and  $\eta = (\eta_1, \dots, \eta_n)^T$  the linear predictor;

- link function (g) that makes the connection between the average of the observations and the systematic part.

$$\eta_i = g(\mu_i)$$

The link function transforms the mean  $\mu_i$  (the mean of  $Y_i$ ) and not the response, that is, the value of the response variable. Thus, there is a great advantage in directly analyzing the model's estimates, thus avoiding a transformation in the estimated values. The GLM class allows the construction of regression models for the parameters of many distributions, such as Binomial, Exponential, Gamma, Weibull, among others.

### 3. Results and discussion

#### 3.1. Sediment characterization

Granulometry (sand, silt and clay) and total organic carbon (TOC) results from sediment sample are shown in [Table 2](#).

Sediment granulometry and TOC content are used to assess the environmental vulnerability to contamination by organic compounds. The fixation of these compounds is associated with the presence of fine sediments, since particles that present small sizes demonstrate a high surface area. Organic matter content can increase the normal flow of organic carbon normally found in mangrove sediments due to oil spills that occur in these environments ([Veiga et al., 2008](#)).

According to [Table 2](#), in the sediment sample silt and clay granulometry are predominant, characterizing a fine sediment. The TOC showed a low percentage. Thus, the accumulation of organic compounds in this sediment sample is governed by granulometry and the low TOC content is an indication that the sediment did not show contamination by organic compounds.

#### 3.2. Photodegradation methodology optimization

To optimize the PAH photodegradation methodology, a factorial design  $2^2$  was used and photocatalyst mass and irradiation time were

**Table 2.** Physical properties of the mangrove sediment sample.

Parameters	Percent
Sand	<DL*
Silt	83.73
Clay	16.27
TOC	0.75

\* Detection Limit - Particles of dimension 2 mm.

evaluated. The lower and upper levels were expressed in [Table 1](#). The photodegradation of seven PAHs (Acenaphthylene (AcNf), Acenaphthene (AcN), Anthracene (AN), Benzo[a]Anthracene (BaA), Indene[1,2,3cd] Pyrene (IP), Dibenz[a,h]Anthracene (DahA), Benzo[ghi]Pyrene (BghiP)) was evaluated, obtaining seven degradation responses.

The photodegradation can be influenced by multiple factors, among them the chemical structure of the organic compound. For aromatic compounds, the amount of aromatic rings in the structure can influence the photodegradation, because the greater the amount of rings, more difficult it will be for the hydroxyl radical to degrade the organic pollutant ([Wick et al., 2011](#)). Because of this, is crucial to find a simultaneous experimental condition to photodegrade low and high molecular weight PAHs. Therefore, the multiple response (MR) was applied to find such an experimental condition. [Eq. 4](#) demonstrates the calculation for obtaining the MR. The values in the denominator of [Eq. 4](#) represent the largest signals obtained for AcNf, AcN, AN, BaA, IP, DahA, BghiP.

$$RM = \frac{AcNf}{95.7} + \frac{AcN}{94.7} + \frac{AN}{72.3} + \frac{BaA}{63.8} + \frac{IP}{65.4} + \frac{DahA}{68.1} + \frac{BghiP}{65.3} \quad (4)$$

According to [Eq. 4](#), each analyte was normalized by its highest value and later the normalized values were added to obtain the MR ([Santos et al., 2009, 2014](#); [Portugal et al., 2007](#); [Ferreira et al., 2003](#)). The application of MR considers multiple responses through a function, observing how changes in factors will affect the responses. This equation normalize the analyze signals to enable a sum of individual responses ([Ferreira, 2015](#)).

The factorial design experiments, was observed that the percentage of photodegradation ranged from 41.9 to 95.7% ([Table 3](#)). Low molecular weight PAHs showed a higher percentage of photodegradation when compared to high molecular weight PAHs. The RM values were used to interpretate the photodegradation from selected PAHs. The experiments 2, 3 and 5 presented the best experimental conditions for the photodegradation. However, experiment 5 (central point values), showed the best experimental conditions for the simultaneous photodegradation of PAHs ([Table 3](#)).

[Dong et al. \(2010\)](#) used 5g of sediment with a variation in the percentage of the mass of the  $TiO_2$  photocatalyst, to degrade phenanthrene and pyrene. Using 2% of  $TiO_2$  (equivalent to 0.1 g in relation to the mass of the sediment), in 25 h of photodegradation, showed 27.5% for phenanthrene and 33.6% for pyrene degradation. The addition of hydrogen peroxide in the same experimental conditions, improve the degradation efficiency to 32.6% for phenanthrene and 38.7% for pyrene. The addition of this reagent provides an increase in the number of hydroxyl radicals, thus favoring a greater efficiency of the photocatalytic process.

According to [Figure 2](#), the photocatalyst mass have no effect in photocatalytic degradation of PAHs, in the design experimental studied. However, low molecular weight PAHs ([Figure 2a, b](#)) showed high degradation when compared to high molecular weight PAHs ([Figure 2c, d](#)). This fact demonstrates that the photocatalytic degradation process is taking place even without the photocatalyst influence. The photochemical behavior of PAHs proved to be dependent on their size and chemical structure. Therefore, the distribution of electrons in the PAHs molecules indicates the reactive sites that can be attacked in photocatalytic oxidation ([Woo et al., 2009](#)).

Pareto chart ([Figure 3](#)) show that the effects of the factors evaluated (mass of the photocatalyst and irradiation time) and the interaction of the factors were not significant for the photodegradation, in the studied domain.

ANOVA test ([Table 4](#)) demonstrated that the mathematical modeling proposed by the central composite planning was a significant regression, at 0.05 significance level, and that there was no lack of fit. Therefore, the best condition for photocatalytic degradation developed is 0.5g photocatalyst and 12 h irradiation time.

#### 3.3. Kinetic parameters

The kinetic parameters of PAHs are demonstrated for the initial concentration of PAHs ( $mg\ kg^{-1}$ ), pseudo-first order constant (k), the



**Table 3.** Coded levels, actual values, percentage of degradation of PAHs and multiple response (MR) obtained in factorial design  $2^2$  with triplicate of the central point, for the evaluation of PAHs photo degradation using  $\text{TiO}_2$ .

Mass of $\text{TiO}_2$ (g)	Irradiation time (h)	Photo degradation (%)							
		AcNf	AcN	A N	BaA	IP	DahA	BghiP	MR
-1 (0.2)	-1 (10)	94.2	92.8	57.4	41.9	46.4	51.3	47.6	5.6
1 (0.8)	-1 (10)	84.7	82.1	62.9	59.9	60.4	65.0	63.5	6.3
-1 (0.2)	1 (14)	95.7	94.7	70.7	55.5	58.2	61.8	61.0	6.5
1 (0.8)	1 (14)	87.1	83.5	58.9	51.5	52.0	55.5	54.5	5.9
0 (0.5)	0 (12)	93.3	91.7	72.3	63.8	65.4	68.1	65.3	6.9
0 (0.5)	0 (12)	88.5	85.4	54.3	45.6	45.7	49.3	48.6	5.3
0 (0.5)	0 (12)	92.0	89.7	67.2	58.9	58.0	61.6	60.8	6.5

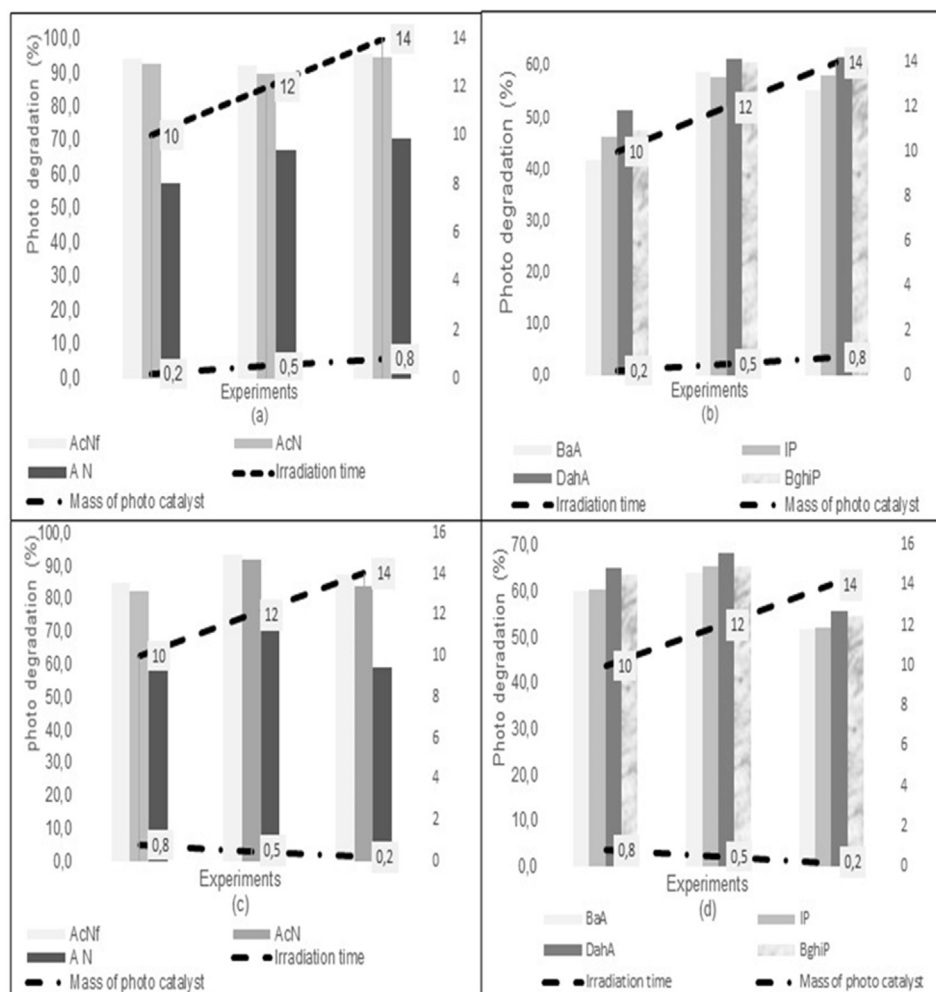
Acenaphthylene (AcNf), Acenaphthene (AcN), Anthracene (AN), Benz[a]Anthracene (BaA), Indene[1,2,3cd]Pyrene (IP), Dibenz[ah]Anthracene (DahA), Benz[ghi]Pyrene (BghiP).

half-life ( $t_{1/2}$ ) and the determination coefficient ( $R^2$ ), as shown in Table 5. With the linearization of Eq. (2) it was possible to find the pseudo-first order constant (k) through the slope and calculate the half-life.

According to the velocity constant values expressed in Table 5, it was possible to observe that the low molecular weight PAHs had the lowest values for the velocity constant when compared to the high molecular weight PAHs. Similar results were found by Zhang et al. (2008) performing PAHs degradation tests using  $\text{TiO}_2$ . Vela et al. (2012) and El-Saeid et al. (2015) observed similar behavior applying photolysis tests.

The half-life express how long the concentration of an organic substance will persist in the environment under the volatilization and/or degradation effects, that is, the time necessary for the initial concentration of PAHs to reach half. The half-life of the compounds determined varied between 3.51 to 9.37 h, and the compounds AcNf and AcN (low molecular weight) had the shortest half-life when compared to those with high molecular weight (Table 5).

Analyzing Figure 4, it can be seen that the half-life with the pseudo-first order kinetic constant and initial PAHs concentration has a negative

**Figure 2.** Analysis of the percentage variation of low molecular weight (a and c) and high molecular weight (b and d) PAHs at the low, high levels and central point for the photo degradation process.

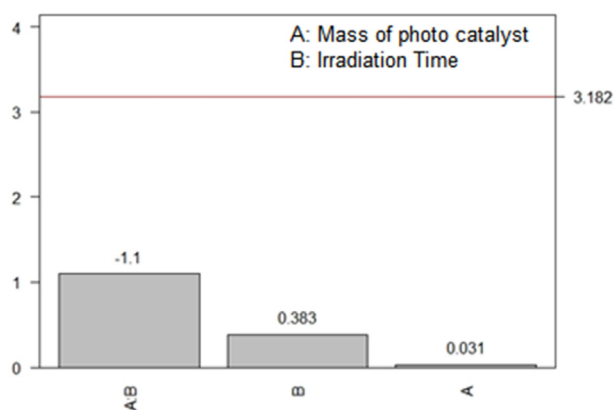


**Figure 3.** Pareto chart for standardized effects for the photo degradation of PAHs considering the MR response variable (Multiple Response).

correlation that is, these variables are inversely proportional. This fact is probably related to the decrease in the available active sites of the catalyst so that the organic compound present in the reaction medium can adsorb (Mills, 2012).

### 3.4. Photocatalytic degradation and photolysis of PAHs

The methods of heterogeneous photocatalysis and photolysis were applied in a sediment contaminated with a reference solution of PAHs and in the sediment contaminated by petroleum, after the spill simulation using the optimized experimental conditions. With these experiments, it was possible to evaluate the photooxidation processes in presence and absence of  $\text{TiO}_2$ , and the study was centered on the aromatic fraction of crude oil from the Potiguar basin. Figures 5 and 6 show the percentages of photooxidation in the presence and absence of the photocatalyst for the reference solution and aromatic fraction of crude oil.

In the reference solution, heterogeneous photocatalysis was more efficient than photolysis, with photodegradation range 92.2–99.5%

(Figure 5) and 93.24% average photodegradation. This results was attributed to the generation of reactive species on the semiconductor surface, mainly the hydroxyl radical. Photolysis had 41.33 average degradation, but Acenaphtene (AcNf) and Acenaphtene (AcN) indicated highest results 91.3 and 65.5%, respectively. PAHs absorb electromagnetic radiation in the ultraviolet region greater than 300 nm and many of them are rapidly photo-oxidized (Lopes and Andrade, 1996). This fact explains the high degradation of these organic compounds in photolysis.

In crude oil aromatic fraction, the photooxidation average was 51.57% with photocatalyst and 61.41% in its absence. However, photolysis was more efficient for AcNf, AcN, AN, DahA, BghiP compounds, with degradation average 86.2, 84.9, 63.3, 59.8 and 65.1, respectively (Figure 6).

The chemical composition of oil is extremely complex with a variety of organic compounds that absorb electromagnetic radiation from the ultraviolet region to the near infrared, passing through the visible (Nicodem et al., 2001). Thus, the wavelength range in the ultraviolet region of sunlight can stimulate the degradation of PAHs in  $\text{TiO}_2$  presence or absence (Chien et al., 2011).

Another important point was that the photodegradation process occurs on the surface of the photocatalyst (or semiconductor), since the molecules of the organic pollutant occupy the active sites of  $\text{TiO}_2$ . This effect is common in photocatalytic processes, as the mechanism involves the adsorption of the compounds to be photodegraded on the surface of the photocatalyst, in higher concentrations it is possible that all active sites are occupied, limiting the adsorption/photodegradation process (Dallago et al., 2009; Herrmann, 1999; Konstantinou and Albanis, 2004). According to Ziolli and Jardim (2002) the efficiency of the photocatalytic process can be affected by the complexity of the sample. Crude oil has a variety of organic compounds and may be competition between them for active sites.

To verify the difference between photocatalytic degradation and photolysis, Kruskal Wallis nonparametric test was applied, which verifies that two or more medians are equal with a 5% significance level. The Shapiro Wilk test indicated that the results do not follow a normal distribution ( $p$ -value  $< 0.05$ ), which justifies the application of this nonparametric test. Table 6 shows the values for the Kruskal

**Table 4.** Analysis of variance for the linear model adjusted to multiple response to a 95% confidence level.

Parameters	Df	QS	SA	$F_{\text{calc}}$	$F_{\text{tab}}$	p-value
A, B	2	0.07	0.03	0.07	19.25	0.93
Residues	4	1.86	0.47			
Lack of adjustment	2	0.60	0.30	0.47	19.00	0.68
Error pure	2	1.27	0.63			

A = mass of photo catalyst, B = irradiation time, Df = degree of freedom, QS = quadratic sum, SA = square average,  $F_{\text{calc}}$  = calculated F test value,  $F_{\text{tab}}$  = tabulated F test value.

**Table 5.** First order constant (k), half-life ( $t_{1/2}$ ) and determination coefficient ( $R^2$ ) for the photo degradation of PAHs with  $\text{TiO}_2$  ( $\lambda = 365\text{nm}$ ).

Compound	$*C_0$	k	$t_{1/2}$	$R^2$
AcNf	0.595	0.1973	3.51	0.9852
AcN	0.592	0.1172	5.91	0.9354
A N	0.569	0.0979	7.08	0.9858
BaA	0.525	0.0816	8.49	0.9628
IP	0.485	0.0740	9.37	0.9856
DahA	0.527	0.0881	7.87	0.9837
BghiP	0.501	0.0764	9.07	0.9849

Acenaphtilene (AcNf), Acenaphtene (AcN), Anthracene (AN), Benz[a]Anthracene (BaA), Indene[1,2,3cd]Pyrene (IP), Dibenz[ah]Anthracene (DahA), Benz[ghi]Pyrene (BghiP).

\* Initial Concentration of the PAHs.

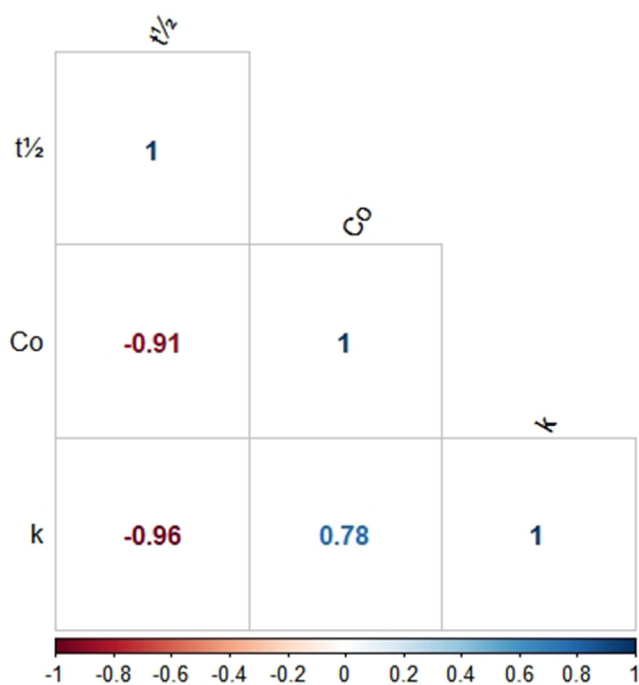


Figure 4. Spearman's correlation graph for kinetic parameters.

Wallis test for the reference solution and aromatic fraction of crude oil.

In PAHs reference solution, nonparametric test (Table 6) indicated a difference between two photooxidation processes, due to the p value being less than the 5% significance level. In order to explore the difference between the heterogeneous photocatalysis and photolysis processes, a Nemenyi multiple comparison test was applied, which is a nonparametric alternative to the Tukey test (Table 7), with the initial concentration of PAHs as the reference for this analysis. However, in the aromatic fraction of crude oil, the photodegradation processes did not show a statistically significant difference (p-value > 0.05), that is, there is not enough evidence to reject the null hypothesis,  $H_0$ , this means that the processes were acting together.

With the results shown in Table 7, it was possible to note significant difference between the initial concentration of the analytes with the heterogeneous photocatalysis process. However, there is no evidence of a significant difference between the photolysis process and the initial concentration of PAHs. Therefore, this fact shows an indication that the irradiation time was not enough to obtain a significant percentage for the degradation of the analytes under study in the absence of the photocatalyst.

### 3.5. Modeling of photo-oxidation processes

The generalized linear model (GLM) was proposed to evaluate the association of the photooxidation in the presence and absence of the photocatalyst applied in the reference solution. The results were modeled using the Gamma distribution due to the values being asymmetric on the right and positive continuums and the link function was identity. The purpose of the link function in the model is to associate the mean of the response variable with the linear predictors of the model.

The regression structure used describes the relationships between the photo-oxidation processes in relation to the gross value of the concentration of aromatic organic compounds. Table 8 shows the estimates, standard error and p-value for the proposed model.

The corrected estimate (Table 8) was found using the logarithmic function that is inverse of the exponential function, since the Gamma distribution belongs to the exponential family. In this way, it is possible to evaluate the photodegradation in PAH solution.

According to Table 8, the photodegradation of PAHs processes were significant at 95% confidence level. Through the analysis of the corrected estimates for the presented model it was possible to verify that the heterogeneous photocatalysis and photolysis are significantly different, reducing 2.78% and 2.405 of the analytes, respectively. The standard error shown in Table 8 is associated with each of the model's estimates. These values were small, thus indicating that there was little variation between the observations. The pseudo  $R^2$  indicates the best fit for the model, because the closer to one this value the better the fit of the model. Thus, pseudo  $R^2$  was 0.751 and the proposed model can explain 75.1% of the data from the photocatalytic process in reference solution.

The adjustment of the final model with gamma distribution is measured by the envelopes simulated graphic (Figure 7). This graph is a

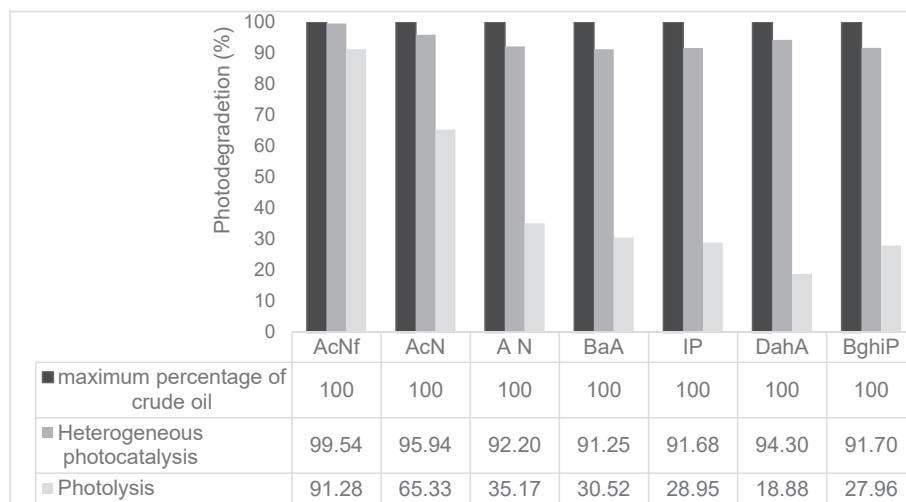
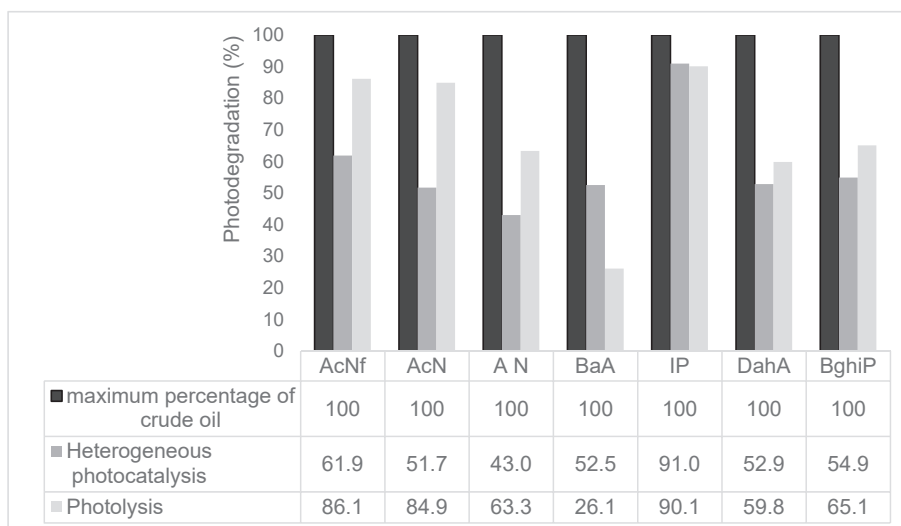


Figure 5. Photo-oxidation process of the PAHs solution in the presence and absence of the  $TiO_2$  photo catalyst. Acenaphthilene (AcNf), Acenaphthene (AcN), Anthracene (AN), Benz[a]Anthracene (BaA), Indene[1,2,3cd]Pyrene (IP), Dibenz[ah]Anthracene (DahA), Benz[ghi]Pyrene (BghiP).



**Figure 6.** Photo-oxidation process of the aromatic fraction of oil from the Potiguar basin in the presence and absence of the TiO<sub>2</sub> photo catalyst. Acenaphthilene (AcNf), Acenaphthene (AcN), Anthracene (AN), Benz[a]Anthracene (BaA), Indene[1,2,3cd]Pyrene (IP), Dibenz[ah]Anthracene (DahA), Benz[ghi]Pyrene (BghiP).

**Table 6.** Nonparametric test applied in the comparison of photo-oxidation processes applied in the standard solution of PAHs and in crude oil.

	Reference solution			Aromatic fraction		
	*Df	Chi-square	p-value	*Df	Chi-square	p-value
Crude oil	2	14.18	0.0008	2	4.03	0.133
Photo catalysis	2	14.18		2	4.03	
Photolysis	2	14.18		2	4.03	

\* Df = degree of freedom.

**Table 7.** Result of the Nemenyi multiple comparison test to ascertain the difference between the photooxidation processes in the standard PAHs solution.

Comparison	p-value
Crude oil versus Photocatalysis	0.0005
Crude oil versus Photolysis	0.267
Photocatalysis versus Photolysis	0.071

visual aid to assess the adequacy of the adjusted model. For the proposed model to have a good fit, it is expected, in this type of graph, that the residues are between the limits of the envelope (Cook and Weisberg, 1999).

According to Figure 7 it can be seen that the residues are dispersed between the limits of the envelope inside. The graph does not point out a serious departure from the assumptions inherent in the model. Therefore, the final model adequately adjusts the data, that is, it provides a good fit.

**Table 8.** Estimates of the explanatory variables selected for the final model.

Parameter	Estimate	Corrected estimate	Standard error	p-value
Intercept	648.6	2.81	118.0	$3.20 \times 10^{-5}$
Photo catalysis	-606.6	-2.78	118.2	$6.99 \times 10^{-5}$
Photolysis	-254.0	-2.40	138.1	0.082
Pseudo-R <sup>2</sup>	0.751			

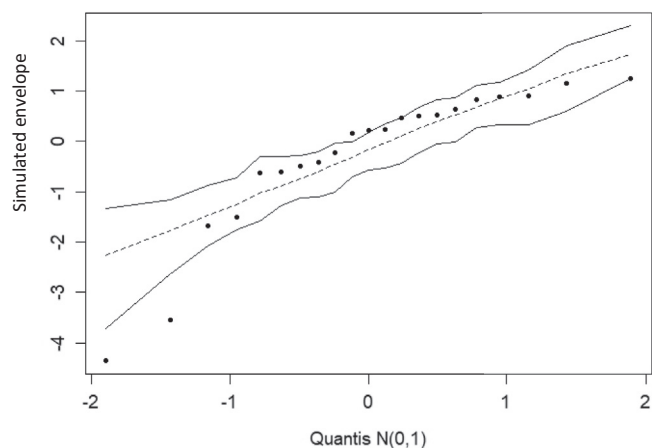


**Figure 7.** Simulated envelope graph for the model adjusted for the variable of interest (Photo degradation).

#### 4. Conclusions

It was found that the interaction of organic compounds in sediment sample is due to the predominance of fine granulometry (silt and clay).

With the Pareto chart it was possible to verify that the isolated factors and their interaction were not significant at the levels studied. The analysis of variance (ANOVA) did not indicate lack of fit for the linear model, with the highest MR value being selected (experiment 5). The optimized experimental conditions were applied to find the kinetic parameters (pseudo-first order constant and half-life time). These parameters indicated that the lower molecular weight PAHs showed the best values for these parameters when compared to high molecular weight.

The optimized experimental conditions were applied to crude oil and a reference solution of PAHs to evaluate the photodegradation of aromatic compounds and also to compare the processes of photocatalysis and photolysis.

The non-parametric statistical test indicated a significant difference between heterogeneous photocatalysis and photolysis for the PAHs standard solution. In this way, a regression model was proposed which



describes the relationship between the two photooxidation processes for the degradation of PAHs. However, for the aromatic fraction, the nonparametric test did not show any significant difference between the degradation processes, therefore, new studies are suggested to understand how these processes act in a complex matrix, which is crude oil. As the results of the reference solution were quite different compared to crude oil, a model was proposed to verify the degree of association of these processes in the photodegradation of PAHs and heterogeneous photocatalysis had a greater association. Therefore, heterogeneous photocatalysis is a promising remediation technique to degrade aromatic organic compounds in mangrove sediments, but it is a complex system that requires more detailed studies regarding its physical and chemical parameters.

## Declarations

### Author contribution statement

Marcio J. Silva: Conceived and designed the experiments; Performed the experiments; Wrote the paper.

Sarah A. R. Soares: Performed the experiments; Analyzed and interpreted the data; Contributed reagents, materials, analysis tools or data; Wrote the paper.

Ingrid D. F. Santos: Performed the experiments; Analyzed and interpreted the data.

Iuri M. Pepe, Leandro R. Teixeira, Lucas Gomes Teixeira, Lucas B. A. Silva@ Contributed reagents, materials, analysis tools or data.

Joil J. Celino: Conceived and designed the experiments; Analyzed and interpreted the data; Wrote the paper.

### Funding statement

This research did not receive any specific grant from funding agencies in the public, commercial, or not-for-profit sectors.

### Competing interest statement

The authors declare no conflict of interest.

### Additional information

No additional information is available for this paper.

## Acknowledgements

This research was carried out in association with the ongoing R&D project registered as ANP N°20075-8, "Research Project for Petroleum Systems in Brazilian Sedimentary Basins" (UFBA/Shell Brazil/ANP), sponsored by Shell Brazil through the "Investment Commitment with Research and Development". We also had the support of the Coordination for the Improvement of Higher Education Personnel - Brazil (CAPES) - Financing Code 001.

## References

- Abdel-Shafy, H.I., Mansour, M.S.M., 2016. A review on polycyclic aromatic hydrocarbons: source, environmental impact, effect on human health and remediation. *Egypt. J. Petrol.* 25, 107–123.
- Ahmed, S., Rasul, M.G., Martens, W.N., Brown, R., Hashib, M.A., 2011. Advances in heterogeneous photocatalytic degradation of phenols and dyes in wastewater: a review. *Water Air Soil Pollut.* 215, 3–29.
- Ambrosio, E., Lucca, D.L., Garcia, M.H.B.M., Souza, T.F., Freitas, T.K.F.S., Souza, R.P., Visentainer, J.V., Garcia, J.C., 2017. Optimization of photocatalytic degradation of biodiesel using TiO<sub>2</sub>/H<sub>2</sub>O<sub>2</sub> by experimental design. *Sci. Total Environ.* 581–582, 1–9.
- Andrade Neto, N.F., Garcia, L.M.P., Longo, E., Li, M.S., Paskocimas, C.A., Bomio, M.R.D., Motta, F.V., 2017. Photoluminescence and photocatalytic properties of Ag/AgCl synthesized by sonochemistry: statistical experimental design. *J. Mater. Sci. Mater. Electron.* 28, 12273–12281.
- Balmer, M.E., Goss, K., Schwarzenbac, R.P., 2000. Photolytic transformation of organic Pollutants on soil surfaces an experimental approach. *Environ. Sci. Technol.* 34, 1240–1245.
- Barka, N., Abdennouri, M., Boussaoud, A., Galadi, A., Baalala, M., Bensitel, M., Sahibed-Dine, A., Nohair, K., Sadiq, M., 2014. Full factorial experimental design applied to oxalic acid photocatalytic degradation in TiO<sub>2</sub> aqueous suspension. *Arab. J. Chem.* 7, 752–757.
- Bolden, A., Rochester, J.R., Schultz, K., Kwiatkowski, S.F., 2017. Polycyclic aromatic hydrocarbons and female reproductive health: a scoping review. *Reprod. Toxicol.* 73, 61–74.
- Calado, V., Montgomery, D.C., 2003. Planejamento de experimentos usando Statistica. E-Papers Serviços Editoriais, Rio de Janeiro, pp. 9–41.
- Chien, S.W.C., Chang, C.H., Chen, S.H., Wang, M.C., Rao, M.M., Veni, S.S., 2011. Effect of sunlight irradiation on photocatalytic pyrene degradation in contaminated soils by micro-nano size TiO<sub>2</sub>. *Sci. Total Environ.* 409, 4101–4108.
- Cook, R., Weisberg, S., 1999. *Applied Regression Including Computing and Graphics*. John Wiley, New York.
- Cordeiro, G.M., Andrade, M.G., 2009. Transformed generalized linear models. *J. Stat. Plann. Inference* 139, 2970–2987.
- Cox, D.R., Reid, N., 2000. *The Theory of the Design Experiments*. Chapman & Hall/CRC, New York, USA.
- Dallago, R.M., Domenech, F., Reolon, J., Di Luccio, M., Egues, S.M.S., 2009. Estudo da degradação fotocatalítica de dimetil dissulfeto: avaliação estatística do efeito do pH da temperatura e concentração do contaminante orgânico. *Quim. Nova* 32 (2), 343–347.
- Dong, D., Li, P., Li, X., Xu, C., Gong, D., Zhang, Y., Zhao, Q., Li, P., 2010. Photocatalytic degradation of phenanthrene and pyrene on soil surfaces in the presence of nanometer rutile TiO<sub>2</sub> under UV-irradiation. *Chem. Eng. J.* 158, 378–383.
- Eguchi, S., 2017. Model comparison for generalized linear models with dependent observations. *Econom. Stat.* 1–18.
- El-Saeid, M.H., Al-Turk, A.M., Nadeem, M.E.A., Hassani, A.S., Al-Wabel, M.I., 2015. Photolysis degradation of polyaromatic hydrocarbons (PAHs) on surface sandy soil. *Environ. Sci. Pollut. Control Ser.* 22, 9603–9616.
- EMBRAPA, 2017. In: Centro Nacional de Pesquisa de solos. Manual de métodos de análise de solo, 3. ed. Embrapa-CNPq, ver. atual. Rio de Janeiro.
- Ferreira, S.L.C., Bezerra, M.A., Santos, W.N.L., Neto, B.B., 2003. Application of Doehlert designs for optimization of an on-line preconcentration system for copper determination by flame atomic absorption spectrometry. *Talanta* 61, 295–303.
- Ferreira, S.L.C., 2015. Introdução às técnicas de planejamento de experimentos, 1ª Ed. Vento Leste, pp. 29–64.
- Gaya, U.I., Abdullah, A.H., 2008. Heterogeneous photocatalytic degradation of organic contaminants over titanium dioxide: a review of fundamentals, progress and problems. *J. Photochem. Photobiol. C Photochem. Rev.* 9, 1–12.
- Gracindo, A.P.A.C., Lara, I.A.R., Façanha, D.A.E., Perreira, G.F., 2011. Estudo do relacionamento do número de bactérias no leite caprino com praticas de higiene via modelos lineares generalizados. *Revista Brasileira de Biometria* 29 (4), 688–698.
- Gupta, H., Gupta, Bina, 2015. Photocatalytic degradation of polycyclic aromatic hydrocarbon benzo[a]pyrene by iron oxides and identification of degradation products. *Chemosphere* 138, 924–931.
- Guz, R., Moura, C., Cunha, M.A.A., Rodrigues, M.B., 2017. Factorial design application in photocatalytic wastewater degradation from TNT industry—red water. *Environ. Sci. Pollut. Control Ser.* 24, 6055–6060.
- Herrmann, J., 1999. Heterogeneous photo catalysis: fundamentals and applications to the removal of various types of aqueous pollutants. *Catal. Today* 53, 115–129.
- Jia, H., Zhao, J., Fan, X., Dilimulati, K., Wang, C., 2012. Photodegradation of phenanthrene on cation-modified clays under visible light. *Appl. Catal. B Environ.* 123–124, 43–51.
- Konstantinou, I.K., Albanis, T.A., 2004. TiO<sub>2</sub>-assisted photocatalytic degradation of azo dyes in aqueous solution: kinetic and mechanistic investigations: a review. *Appl. Catal. B Environ.* 49, 1–14.
- Kuppusamy, S., Thavamani, P., Venkateswarlu, K., Lee, Y.B., Naidu, R., Mgaharaf, M., 2017. Remediation approaches for polycyclic aromatic hydrocarbons (PAHs) contaminated soils: technological constraints, emerging trends and future directions. *Chemosphere* 168, 944–968.
- Lopes, W.A., Andrade, J.B., 1996. Fontes, formação, reatividade e quantificação de hidrocarbonetos policíclicos aromáticos (HPA) na atmosfera. *Quím. Nova* 19, 497–516.
- Marquês, M., Mari, M., Audí-Miró, C., Sierra, J., Soler, A., Nadal, M., Domingo, J.L., 2016. Climate change impact on the PAH photodegradation in soils: characterization and metabolites identification. *Environ. Int.* 89–90, 155–165.
- Mills, A., 2012. An overview of the methylene blue ISO test for assessing the activities of photocatalytic films. *Appl. Catal. B Environ.* 128, 144–149.
- Mishra, A., Mehta, A., Sharma, M., Basu, S., 2017. Enhanced heterogeneous photodegradation of VOC and dye using microwave synthesized TiO<sub>2</sub>/Clay nanocomposites: a comparison study of different type of clays. *J. Alloys Compd.* 694, 574–580.
- Nelder, J.A., Wedderburn, R.W.M., 1972. Generalized linear models. *J. Roy. Stat. Soc.* 135, 370–384.
- Novaes, C.G., Yamaki, R.T., De Paula, V.F., Do Nascimento Júnior, B.B., Barreto, J.A., Valasques, G.S., Bezerra, M.A., 2017. Otimização de métodos analíticos usando metodologia de superfícies de resposta - Parte I: Variáveis de processo. *Revista virtual de química* 9.
- Nicodem, D.E., Fernandes, M.C.Z., Guedes, C.L.B., Correa, R.J., Severino, D., Coutinho, M., Silva, J., 2001. Photochemistry of petroleum. *Prog. React. Kinet. Mech.* 26, 219–238.

- Nugraha, J., Fatimah, I., 2013. Evaluation of photodegradation efficiency on semiconductor immobilized clay photocatalyst by using probity model approximation. *Int. J. Chem. Anal. Sci.* 4, 125–130.
- Pohlert, T., 2014. The Pairwise Multiple Comparison of Mean Ranks Package (PMCMR). R Package. Available in: <https://CRAN.R-project.org/package=PMCMR>.
- Portugal, L.A., Ferreira, H.S., Santos, W.N.L., Ferreira, S.L.C., 2007. Simultaneous pre-concentration procedure for the determination of cadmium and lead in drinking water employing sequential multi-element flame atomic absorption spectrometry. *Microchem. J.* 87, 77–80.
- R Development Core Team, 2019. R: A Language and Environment for Statistical Computing. R Foundation for Statistical Computing. Version 3.6.0 Available in: <http://www.R-project.org>. (Accessed 17 November 2018).
- RStudio Team, 2015. RStudio: Integrated Development for R. RStudio, Inc. Version 1.1.463. Available in: <http://www.r-qualitytools.org>. (Accessed 17 November 2018).
- Roth, T., 2016. Quality Tools: Statistics in Quality Science. R Package Version 1.55. Available in: <http://www.r-qualitytools.org>.
- Santos, D.C.M.B., Carvalho, L.S.B., Lima, D.C., Leão, D.J., Teixeira, L.S.G., Korn, M.G.A., 2014. Determination of micronutrient minerals in coconut milk by ICP OES after ultrasound-assisted extraction procedure. *J. Food Compos. Anal.* 34, 75–80.
- Santos, W.P.C., Castro, J.T., Bezerra, M.A., Fernandes, A.P., Ferreira, S.L.C., Korn, M.G.A., 2009. Application of multivariate optimization in the development of an ultrasound-assisted extraction procedure for multielemental determination in bean seeds samples using ICP OES. *Microchem. J.* 91, 153–158.
- Singh, L., Varshney, J.G., Agarwal, T., 2016. Polycyclic aromatic hydrocarbons' formation and occurrence in processed food. *Food Chem.* 199, 768–781.
- US EPA, 2007a. United States Environmental Protection Agency: Method 3546 - Microwave Extraction.
- US EPA, 2007b. United States Environmental Protection Agency: Method 8270 D - Semi Volatile Organic Compound by Gas Chromatography/mass Spectrometry (GC-MS).
- Veiga, I.G., Triguês, J.A., Celino, J.J., Oliveira, O.M.C., 2008. Hidrocarbonetos saturados em sedimentos de manguezais na área norte da Baía de Todos os Santos. In: Queiroz, A.F.S., Celino, J.J., coordenadores) (Eds.), Avaliação de ambientes na Baía de Todos os Santos: aspectos geoquímicos, geofísicos e biológicos. Salvador: UFBA, pp. 149–187.
- Vela, N., Martínez-Menchón, M., Navarro, G., Pérez-Lucas, G., Navarro, S., 2012. Removal of polycyclic aromatic hydrocarbons (PAHs) from groundwater by heterogeneous photocatalysis under natural sunlight. *J. Photochem. Photobiol. A Chem.* 232, 32–40.
- Virgillito, S.B., 2006. Estatística Aplicada, 3ª Ed. rev. e ampl. Edicon, São Paulo.
- Wick, A.F., Daniels, W.L., Tech, V., 2011. Remediation of PAH-Contaminated Soils and Sediments: A Literature Review Environmental Soil Science, Wetland Restoration and Mined Land Reclamation, pp. 2–102.
- Woo, O.T., Chung, W.K., Wong, K.H., Chow, A.T., Wong, P.K., 2009. Photocatalytic oxidation of polycyclic aromatic hydrocarbons: intermediates identification and toxicity testing. *J. Hazard Mater.* 168, 1192–1199.
- Zhang, L., Li, P., Gong, Z., Li, X., 2008. Photocatalytic degradation of polycyclic aromatic hydrocarbons on soil surfaces using TiO<sub>2</sub> under UV light. *J. Hazard Mater.* 158, 478–484.
- Zioli, R.L., Jardim, W.F., 2002. Photocatalytic decomposition of seawater-soluble crude-oil fractions using high surface area colloid nanoparticles of TiO<sub>2</sub>. *J. Photochem. Photobiol. A Chem.* 47, 205–212.